

A Novel Space Vector PWM of Z-Source Inverter with Minimum Inductor Current Ripple

Jyothi Joseph C¹, Salini Menon V² and Sreedevi K P³

¹Thejus Engineering College
Electrical and Electronics Department (Thrissur, Kerala, India)
jyothijosephc1992@gmail.com

²Thejus Engineering College
Electrical and Electronics Department (Thrissur, Kerala, India)
salinimenon.v@gmail.com

³ Thejus Engineering College
Electrical and Electronics Department (Thrissur, Kerala, India)
sreedevikpn@gmail.com

ABSTRACT—*The Z-Source Inverter (ZSI) overcomes the disadvantages of the traditional Voltage-Source Inverter (VSI) and Current-Source Inverter (CSI). It can buck and boost its output voltage by utilizing the shoot-through state which is forbidden in traditional VSI. Different Pulse Width Modulation (PWM) techniques are available for the control of Z-Source Inverters. In the traditional PWM technique equal shoot-through time interval is considered for the three phase legs. Hence, the realization of the shoot-through state is easy, but the main drawback of this modulation method is big inductor ripple and a large inductor when the output frequency is low. In this paper, a novel Space Vector Pulse Width Modulation (SVPWM) technique to reduce the inductor current ripple is proposed, which will minimize the cost and size of the circuit while providing a higher output voltage boost. The principle of the traditional and proposed SVPWM strategy is analyzed, and the comparison of current ripple under the traditional and proposed strategy is given. Simulation and experimental results are shown to verify the analysis.*

Keywords—Current Ripple, Modified Space Vector PWM, Shoot Through, Z-Source Inverter (ZSI)

1. INTRODUCTION

A Z-source inverter can provide unique features that cannot be obtained in traditional voltage–source and current–source inverters. It can buck and boost its output voltage by utilizing the shoot-through state which is forbidden in traditional VSI. In the applications with wide-range input voltage, ZSI can buck and boost voltage, which is achieved by two-stage power converter traditionally. Therefore, it has broad application prospects. A shoot-through state is when the two switches in any of the three phase legs are turned on at the same time. In the three-phase Z-source inverter the Z-source network is used as the front stage and it can provide shoot-through of the phase legs and buck–boost ability, as compared to traditional topologies.

The traditional Z-source inverter (three phase) as shown in Fig. 1, employs a symmetrical LC impedance network to replace the dc-link capacitor in traditional VSI. Furthermore, with the help of series diode embedded in the source side, the input dc source can be effectively disconnected from the Z-source network by naturally reverse-biasing the diode D during the unique shoot-through interval, which can be initiated by turning ON all switches of one phase-leg simultaneously [1]. Such special operation provides the ability of voltage boosting as well as the unidirectional power conversion (desired in PV and fuel cell systems).

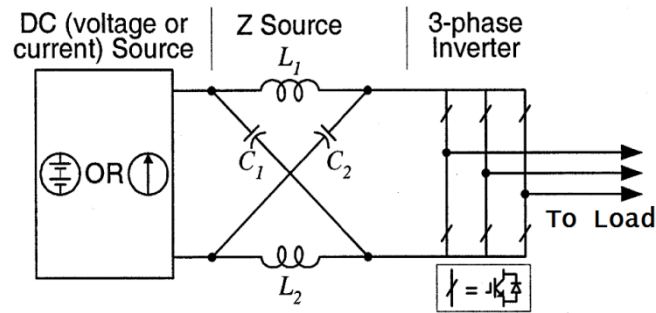


Figure 1: Three Phase Z-Source Inverter

2. EQUIVALENT CIRCUIT & OPERATING PRINCIPLE

The three-phase Z-source inverter bridge has nine permissible switching states or vectors, where the traditional three-phase Voltage source inverter has only eight. The traditional three-phase Voltage source inverter has six active vectors when the dc voltage is impressed across the load and two zero vectors when the load terminals are shorted through either the lower or upper three devices, respectively.

However, the three-phase Z-source inverter bridge has one additional zero state (vector) when the load terminals are shorted through both the upper and lower devices of any one phase leg, any two phase legs, or all three phase legs. This shoot-through zero state (or vector) is forbidden in the traditional Voltage source inverter, because it would cause a shoot-through. This shoot-through zero state provides the unique buck-boost feature to the inverter.

Fig. 2 shows the equivalent circuit of the Z-source inverter shown in Fig. 1 when viewed from the dc link. The inverter bridge is equivalent to a short circuit when the inverter bridge is in the shoot-through zero state, as shown in Fig. 3, whereas the inverter bridge becomes an equivalent current source as shown in Fig. 4 when in one of the six active states. Note that the inverter bridge can be also represented by a current source with zero value (i.e., an open circuit) when it is in one of the two traditional zero states [4]. Therefore, Fig. 4 shows the equivalent circuit of the Z-source inverter viewed from the dc link when the inverter bridge is in one of the eight non-shoot-through switching states.

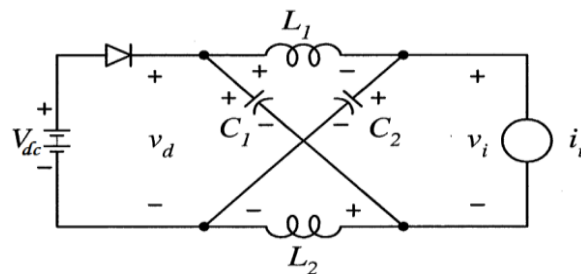


Figure 2: Equivalent Circuit of the ZSI

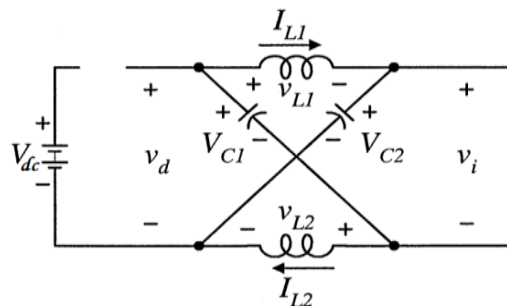


Figure 3: Equivalent Circuit during Shoot-Through State

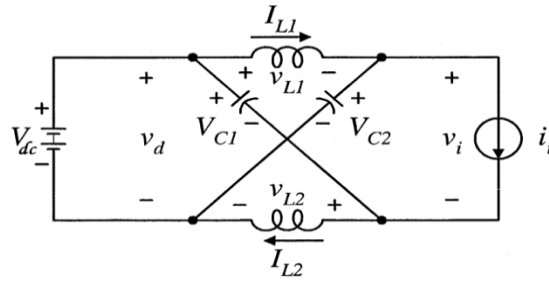


Figure 4: Equivalent Circuit during Non-Shoot-Through State

3. CIRCUIT ANALYSIS

Assuming that the inductors L_1 and L_2 and capacitors C_1 and C_2 have the same inductance, L and capacitance, C respectively; the Z-source network becomes symmetrical [4]-[5]. From the symmetry and the equivalent circuits, we have

$$V_{C1} = V_{C2} = V_C v_{L1} = v_{L2} = v_L \quad (1)$$

Given that the inverter bridge is in the shoot-through zero state for an interval of T_0 , during a switching cycle T , and from the equivalent circuit, Fig. 3, we get,

$$v_L = V_C v_d = 2V_C v_i = 0 \quad (2)$$

Next consider that the inverter bridge is in one of the eight non-shoot-through states for an interval of T_1 , during the switching cycle, T . From the equivalent circuit, Fig. 4, we get,

$$\begin{aligned} v_L &= V_{dc} - V_C v_d = V_{dc} \\ v_i &= V_C - v_L = 2V_C - V_{dc} \end{aligned} \quad (3)$$

Where V_{dc} is the dc source voltage and $T = T_0 + T_1$.

The average voltage of the inductors over one switching period should be zero in steady state, from (2) and (3), thus, we get,

$$V_L = \bar{v}_L = \frac{T_0 \cdot 0 + T_1 \cdot (V_{dc} - V_C)}{T} = 0 \quad (4)$$

or

$$\frac{V_C}{V_{dc}} = \frac{T_1}{T_1 - T_0} \quad (5)$$

Similarly, the average dc-link voltage across the inverter bridge can be found as follows:

$$\begin{aligned} V_i = \bar{v}_i &= \frac{T_0 \cdot 0 + T_1 \cdot (2V_C - V_{dc})}{T} \\ &= \frac{T_1}{T_1 - T_0} V_{dc} = V_C \end{aligned} \quad (6)$$

The peak dc-link voltage across the inverter bridge is expressed in (3) and can be rewritten as,

$$\hat{v}_i = V_C - v_L = 2V_C - V_{dc} = \frac{T}{T_1 - T_0} V_{dc} = B V_{dc} \quad (7)$$

Where,

$$B = \frac{T}{T_1 - T_0} = \frac{1}{1 - \frac{2T_0}{T}} \geq 1 \quad (8)$$

is the boost factor resulting from the shoot-through zero state. The peak dc-link voltage \hat{v}_i , is the equivalent dc-link voltage of the inverter. On the other side, the output peak phase voltage from the inverter can be expressed as,

$$\hat{v}_{ac} = M \cdot \frac{\hat{v}_i}{2} \quad (9)$$

Where M is the modulation index. Using (7), (9) can be further expressed as

$$\hat{v}_{ac} = M \cdot B \cdot \frac{V_{dc}}{2} \quad (10)$$

For the traditional voltage source PWM inverter, we have the well-known relationship, $\hat{v}_{ac} = M \cdot \frac{V_{dc}}{2}$.

Equation (10) shows that the output voltage can be stepped up and down by choosing an appropriate buck–boost factor B_B ,

$$B_B = M \cdot B = (0 \sim \infty) \quad (11)$$

From (1), (5) and (8), the capacitor voltage can be expressed as

$$V_{C1} = V_{C2} = V_C = \frac{1 - \frac{T_0}{T}}{1 - \frac{2T_0}{T}} \cdot V_{dc} \quad (12)$$

The buck–boost factor is determined by the modulation index and boost factor. The boost factor as expressed in (8) can be controlled by duty cycle (i.e., interval ratio) of the shoot-through zero state over the non-shoot-through states of the inverter PWM.

4. TRADITIONAL PWM STRATEGY

The switching sequence of VSI and ZSI with traditional sinusoidal PWM is shown in Fig. 5. By inserting the shoot-through states into the switching transits in VSI, the PWM strategy of ZSI can be derived. There are six shoot-through states T in one carrier period. All shoot-through times are equal.

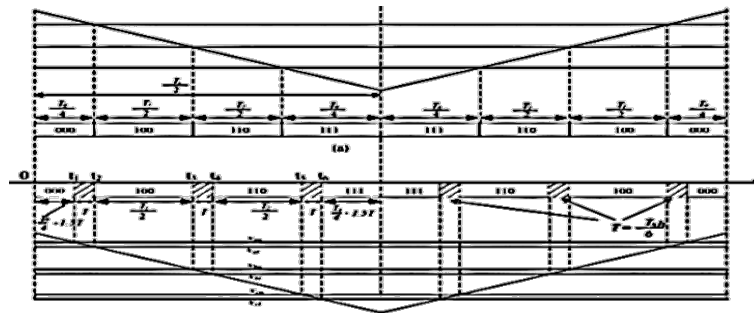


Figure 5: Switching Sequence of VSI and ZSI in Traditional PWM Strategy

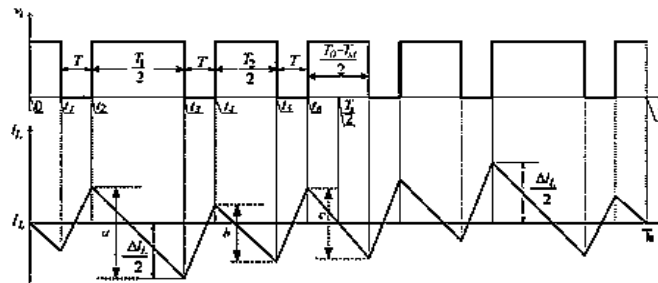


Figure 6: Inductor Current Ripple in Traditional PWM Strategy

Fig. 6 shows the waveform of inductor current ripple. In shoot-through state, the inductor current rises; while in non-shoot-through state, the inductor current decreases [2]-[3].

The inductor current ripple can be expressed as,

$$\Delta i_L = 2 \max(|i(t_1) - I_L|, |i(t_2) - I_L|, |i(t_3) - I_L|, |i(t_4) - I_L|, |i(t_5) - I_L|, |i(t_6) - I_L|) \quad (13)$$

Where, I_L represents the average value of inductor current.

5. PROPOSED SPACE VECTOR PWM STRATEGY

The biggest difference of Space Vector Pulse Width Modulation from other PWM methods is that the SVPWM uses a vector as a reference. This gives the advantage of a better overview of the system. In this proposed SVPWM strategy, first we derive the traditional SVPWM for a Voltage Source Inverter (VSI) and then apply the shoot-through pulses into

the obtained switching sequence. The proposed method can not only minimize the inductor current ripple, it can also provide a higher voltage boost and lesser Inrush current at startup.

The circuit model of a typical three-phase voltage source PWM inverter is shown in Fig. 7. S_1 to S_6 are the six power switches that shape the output, which are controlled by the switching variables a, a', b, b', c, c' .

When an upper transistor is switched ON, i.e., when a, b or c is 1, the corresponding lower transistor is switched OFF, i.e., the corresponding a', b' or c' is 0. Therefore, the ON and OFF states of the upper transistors S_1, S_3 and S_5 can be used to determine the output voltage.

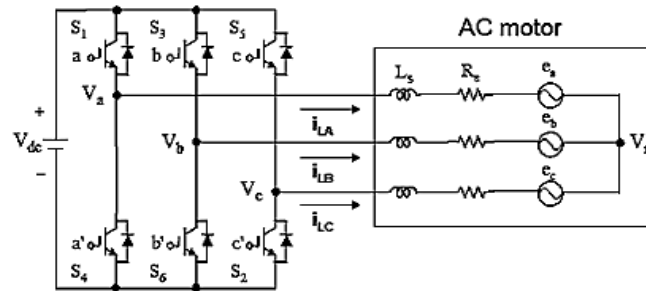


Figure 7: Three Phase Voltage Source PWM Inverter

The relationship between the switching variable vector $[a, b, c]$ and the phase voltage vector $[V_a, V_b, V_c]$ can be expressed below.

$$\begin{bmatrix} V_{an} \\ V_{bn} \\ V_{cn} \end{bmatrix} = \frac{V_{dc}}{3} \begin{bmatrix} 2 & -1 & -1 \\ -1 & 2 & -1 \\ -1 & -1 & 2 \end{bmatrix} \begin{bmatrix} a \\ b \\ c \end{bmatrix} \quad (14)$$

There are eight possible combinations of ON and OFF patterns for the three upper power switches. The ON and OFF states of the lower power devices are opposite to the upper one and so are easily determined once the states of the upper power transistors are determined [6]-[8].

Table 1: Switching vectors, phase voltages and output line to line voltages

Voltage Vectors	Switching Vectors			Line to Neutral Voltage			Line to Line Voltage		
	a	b	c	V_{an}	V_{bn}	V_{cn}	V_{ab}	V_{bc}	V_{ca}
V_0	0	0	0	0	0	0	0	0	0
V_1	1	0	0	$2/3$	$-1/3$	$-1/3$	1	0	-1
V_2	1	1	0	$1/3$	$1/3$	$-2/3$	0	1	-1
V_3	0	1	0	$-1/3$	$2/3$	$-1/3$	-1	1	0
V_4	0	1	1	$-2/3$	$1/3$	$1/3$	-1	0	1
V_5	0	0	1	$-1/3$	$-1/3$	$2/3$	0	-1	1
V_6	1	0	1	$1/3$	$-2/3$	$1/3$	1	-1	0
V_7	1	1	1	0	0	0	0	0	0

Note that the respective voltage should be multiplied by V_{dc} .

According to (14), the eight switching vectors, output line to neutral voltage (phase voltage), and output line-to-line voltages in terms of input DC voltage V_{dc} , are given in Table1.

Space Vector PWM (SVPWM) refers to a special switching sequence of the upper three power transistors of a three-phase power inverter. It has been shown to generate less harmonic distortion in the output voltages and or currents applied to the phases of an AC motor and to provide more efficient use of supply voltage compared with sinusoidal modulation technique. The biggest difference from other PWM methods is that the SVPWM uses a vector as a reference. This gives the advantage of a better overview of the system [8]-[12].

Out of the 8 possible switching states, two are zero switching states and six are active switching states. These are represented by active (V1-V6) and zero (V0) vectors. Six nonzero vectors (V1 - V6) shape the axes of a hexagonal and feed electric power to the load. The angle between any adjacent two non-zero vectors is 60 degrees. Meanwhile, two zero vectors (V0 and V7) are placed at the origin and apply zero voltage to the load. This is shown in Fig. 8.

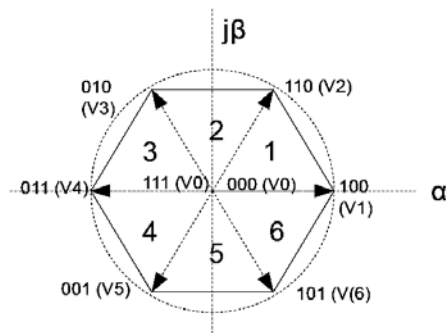


Figure 8: Space Voltage Vectors in Different Sectors

The reference vector is represented in a $\alpha\beta$ -plane shown in Fig. 9. This is a two-dimensional plane transformed from a three-dimensional plane containing the vectors of the three phases. The switches being ON or OFF are determined by the location of the reference vector on this $\alpha\beta$ -plane.

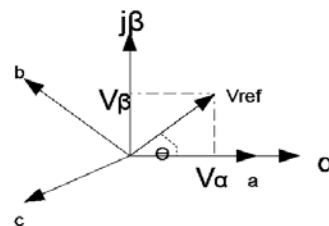


Figure 9: The Reference Vector in the Two and Three Dimensional Plane

The relation between these two reference frames (abc and $\alpha\beta$) is below,

$$f_{\alpha\beta 0} = K_s f_{abc} \quad (15)$$

Where K_s is,

$$K_s = \frac{2}{3} \begin{bmatrix} 1 & -1/2 & -1/2 \\ 0 & \sqrt{3}/2 & -\sqrt{3}/2 \\ 1/2 & 1/2 & 1/2 \end{bmatrix} \quad (16)$$

f denotes either a voltage or a current variable. The magnitude and angle of the reference vector can be calculated with Clark's Transformation:

$$V_{ref} = V_\alpha + jV_\beta = \frac{2}{3}(V_a + aV_b + a^2V_c) \quad (17)$$

Where a is given by

$$a = e^{j\frac{2\pi}{3}} \quad (18)$$

The magnitude and angle (determining in which sector the reference vector is in) of the reference vector is:

$$|V_{ref}| = \sqrt{V_\alpha^2 + V_\beta^2} \quad \theta = \tan^{-1} \left(\frac{V_\beta}{V_\alpha} \right) \quad (19)$$

The voltage vectors on the alpha and beta axis can then be described as:

$$V_\alpha = \frac{2}{3} \left(V_a - \frac{1}{2} V_b - \frac{1}{2} V_c \right)$$

$$V_\beta = \frac{2}{3} \left(\frac{\sqrt{3}}{2} V_b - \frac{\sqrt{3}}{2} V_c \right) \tag{20}$$

The next step is to calculate the duration time for each vector V_1 - V_6 . The switching time duration at any sector can be obtained as follows,

$$T_1 = \frac{\sqrt{3} \cdot T_z \cdot \bar{V}_{ref}}{V_{dc}} \left(\sin \frac{n}{3} \pi \cdot \cos \theta - \cos \frac{n}{3} \pi \cdot \sin \theta \right)$$

$$T_2 = \frac{\sqrt{3} \cdot T_z \cdot \bar{V}_{ref}}{V_{dc}} \left(\cos \theta \cdot \sin \frac{n-1}{3} \pi + \sin \theta \cdot \cos \frac{n-1}{3} \pi \right)$$

$$T_0 = T_z - T_1 - T_2 \quad (0 \leq \theta \leq 60^\circ) \tag{21}$$

Where, n = 1 through 6 (i.e., Sector1 to 6)

Next, the switching time at each sector is summarized in Table 2.

Table 2: Switching time calculation at each sector

Sector	Upper Switches (S_1, S_3, S_5)	Lower Switches (S_4, S_6, S_2)
1	$S_1 = T_1 + T_2 + T_0/2$ $S_3 = T_2 + T_0/2$ $S_5 = T_0/2$	$S_4 = T_0/2$ $S_6 = T_1 + T_0/2$ $S_2 = T_1 + T_2 + T_0/2$
2	$S_1 = T_1 + T_0/2$ $S_3 = T_1 + T_2 + T_0/2$ $S_5 = T_0/2$	$S_4 = T_2 + T_0/2$ $S_6 = T_0/2$ $S_2 = T_1 + T_2 + T_0/2$
3	$S_1 = T_0/2$ $S_3 = T_1 + T_2 + T_0/2$ $S_5 = T_2 + T_0/2$	$S_4 = T_1 + T_2 + T_0/2$ $S_6 = T_0/2$ $S_2 = T_1 + T_0/2$
4	$S_1 = T_0/2$ $S_3 = T_1 + T_0/2$ $S_5 = T_1 + T_2 + T_0/2$	$S_4 = T_1 + T_2 + T_0/2$ $S_6 = T_2 + T_0/2$ $S_2 = T_0/2$
5	$S_1 = T_2 + T_0/2$ $S_3 = T_0/2$ $S_5 = T_1 + T_2 + T_0/2$	$S_4 = T_1 + T_0/2$ $S_6 = T_1 + T_2 + T_0/2$ $S_2 = T_0/2$
6	$S_1 = T_1 + T_2 + T_0/2$ $S_3 = T_0/2$ $S_5 = T_1 + T_0/2$	$S_4 = T_0/2$ $S_6 = T_1 + T_2 + T_0/2$ $S_2 = T_2 + T_0/2$

Next, the required shoot-through pulses can be added. Fig. 10 shows the diagram for adding the shoot-through pulses. The rising and falling edges are first detected and a unit delay is used to apply the shoot-through pulses (i.e. the ON time of switches in the three phase legs are controlled to achieve shoot-through zero state).

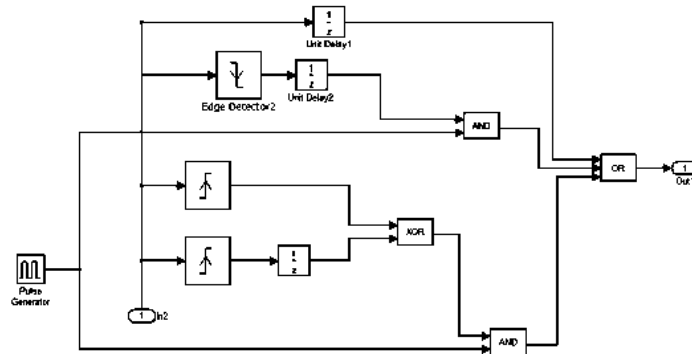


Figure 10: Diagram for Adding Shoot-Through Zero State

6. SIMULATION AND EXPERIMENTAL RESULTS

ZSI is designed with the following parameters,

1. Input voltage V_{dc} : 200 V–400 V;
2. Rated capacity: 3 kVA;
3. Switching frequency: 13.5 kHz;
4. Z-source network: $L = 500 \mu\text{H}$, $C = 2000 \mu\text{F}$;
5. Output filter: $L_f = 1000 \mu\text{H}$, $C_f = 15\mu\text{F}$.

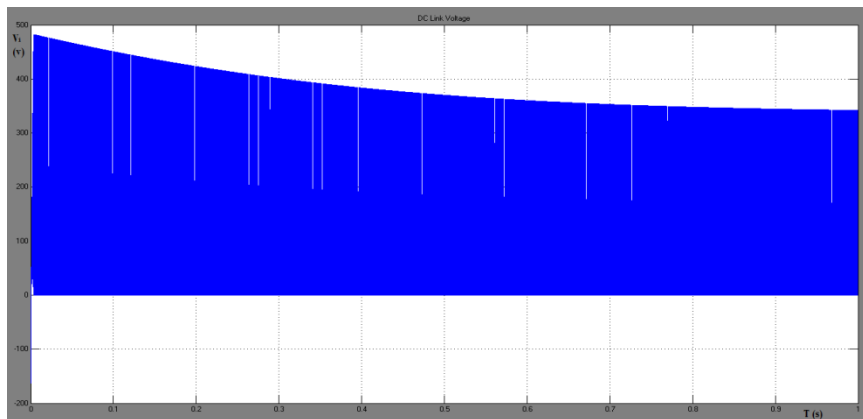


Figure 11: DC Link Voltage from Traditional PWM

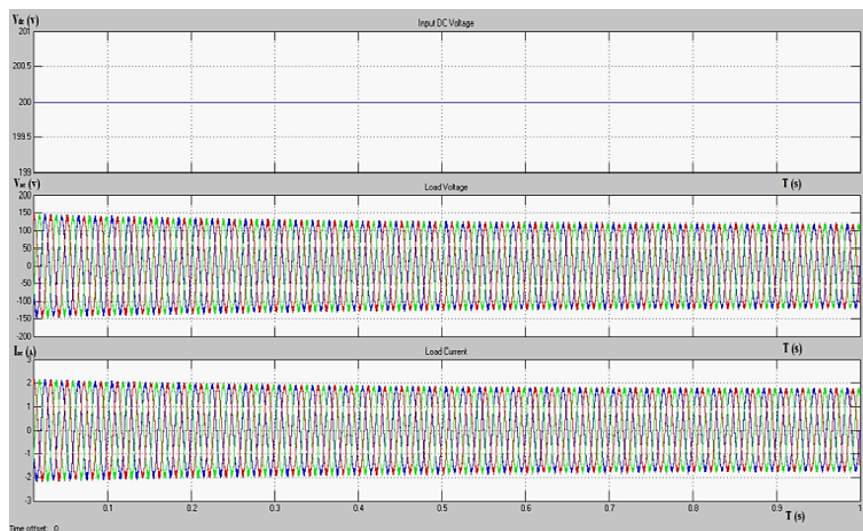


Figure 12: Voltage Waveforms from Traditional PWM

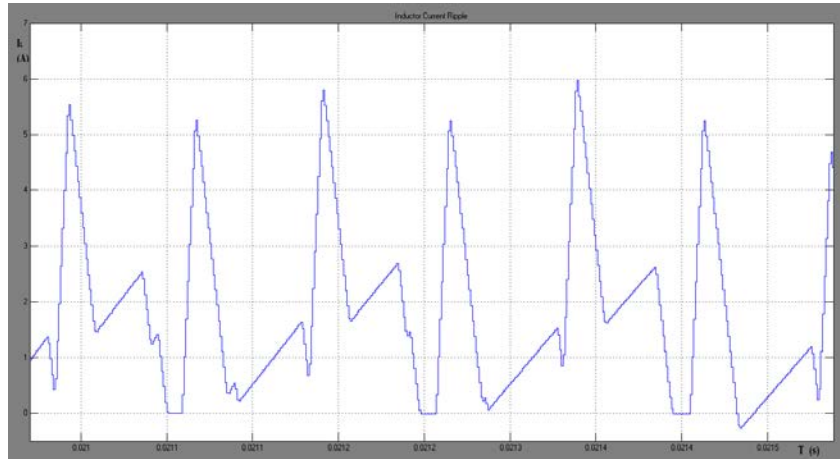


Figure 13: Inductor Current Ripple from Traditional PWM

When $V_{dc} = 200$ V, The boosted dc link voltage, Input and output voltage waveforms are given in Fig. 11, Fig. 12 respectively. The maximum current ripple through the inductor is 6A, this is shown in Fig. 13.

For the same input voltage, The boosted dc link voltage, Input and output voltage waveforms are given in Fig. 14, Fig. 15 respectively. It is clear from Fig. 11 and 14 that a higher dc voltage boost is obtained with the proposed SVPWM. Also the Inductor current ripple has been dramatically reduced to 0.8A in Fig. 16. Another advantage of this proposed SVPWM is that it can reduce the Inrush current at startup.

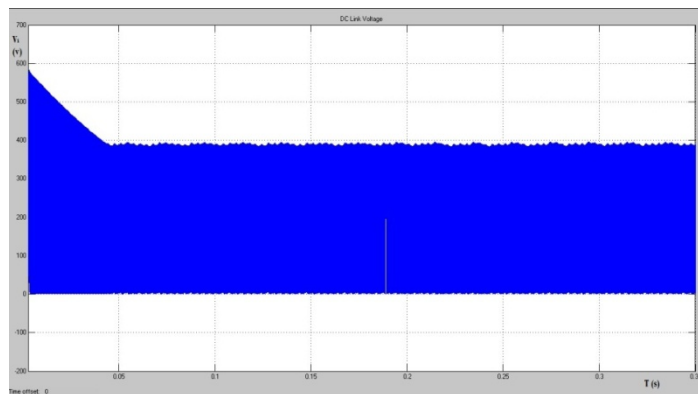


Figure 14: DC Link Voltage from Proposed SVPWM

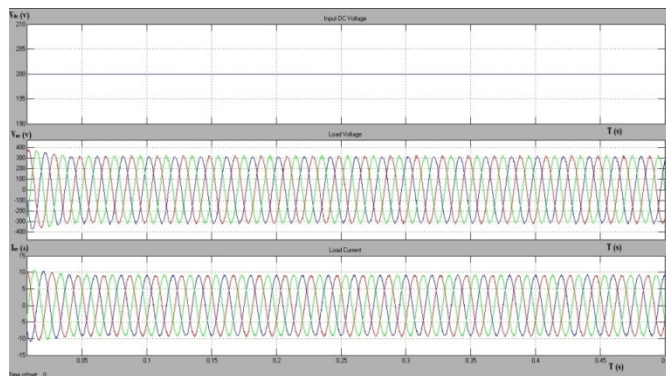


Figure 15: Voltage Waveforms from Proposed SVPWM

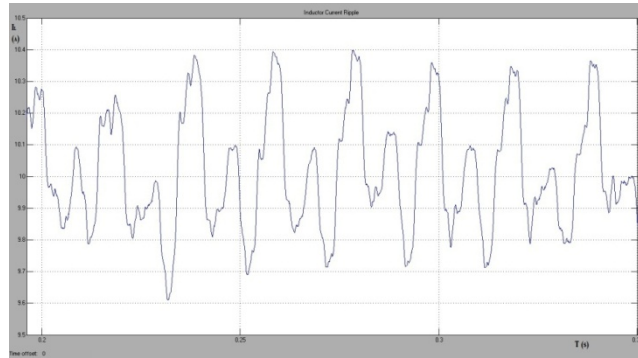


Figure 16: Inductor Current Ripple from Proposed SVPWM

7. CONCLUSION AND FUTURE ENHANCEMENT

The ripple current was analyzed in detail under the existing and new PWM scheme and the realization of the proposed SVPWM scheme was derived. Analysis, simulation, and experimental results reveal that the proposed SVPWM scheme can reduce the ripple current greatly, and thus smaller inductors can be utilized in ZSI. The maximum current ripple through the inductor is 0.8A when compared to the ripple of 6A obtained from traditional method. The proposed SVPWM provides a higher voltage boost when compared to the traditional PWM scheme. ZSI with minimum inductor current ripple is useful in the integration of renewable energy systems. In future, modeling of PV system or any other renewable energy system can be done and the proposed SVPWM can be applied.

8. ACKNOWLEDGMENT

Author thanks Mrs. Sreedevi Bhas, Asst. Professor of Electrical Department at Thejus Engineering College, Vellarakkad and Mrs. Jisi Nalupurakkandiyil, Asst. Professor of Electrical Department at Thejus Engineering College, Vellarakkad for their cordial support, valuable information and guidance.

9. REFERENCES

- [1] Y. Tang, S. Xie, and C. Zhang, "Single-phase Z-source inverter" IEEE Transactions on Power Electronics, Vol. 26, No. 12, Pp. 3869-3873, 2011.
- [2] Yu Tang, Shaojun Xie, and Jiudong Ding "Pulsewidth Modulation of Z-Source Inverters With Minimum Inductor Current Ripple", IEEE Transactions on Industrial Electronics, Vol. 61, No. 1, Pp. 98-106, 2014.
- [3] Penchalababu.V, Chandrakala.B, Gopal Krishna, "A Survey on Modified PWM Techniques for Z-Source Inverter," International Journal of Engineering and Advanced Technology (IJEAT), Volume-1, Issue-5, Pp. 556-562, 2012.
- [4] F. Z. Peng, "Z-source inverter," IEEE Transactions on Industry Applications, Vol. 39, No. 2, Pp. 504-510, 2003.
- [5] M. Shen and F. Z. Peng, "Operation modes and characteristics of the Z-source inverter with small inductance or low power factor," IEEE Transactions on Industrial Electronics, Vol. 55, No. 1, Pp. 89-96, 2008
- [6] Miaosen Shen, Jin Wang, Alan Joseph, Fang Zheng Peng, Leon M. Tolbert, and Donald J. Adams "Constant Boost Control of the Z-Source Inverter to Minimize Current Ripple and Voltage Stress," IEEE Transactions on Industry Applications, Vol. 42, No. 3, Pp. 770-778, 2006
- [7] Poh Chiang Loh, Mahinda Vilathgamuwa, Yue Sen Lai, Geok Tin Chua, and Yunwei Li, "Pulse-Width Modulation of Z-Source Inverters" IEEE Transactions on Power Electronics, Vol. 20, No. 6, Pp. 1346-1355, 2005.
- [8] S. Thangaprakash and A. Krishnan, "Modified Space Vector Pulse Width Modulation for Z-Source Inverters" , International Journal of Recent Trends in Engineering, Vol 2, No. 6, Pp. 136-138, 2009.
- [9] T. Meenakshi and K. Rajambal, "Identification of an Effective Control Scheme for Z-source Inverter", Asian Power Electronics Journal, Vol. 4 No.1, Pp. 22-28, 2010.
- [10] Budi Yanto Husodo, Shahrin Md. Ayob, Makbul Anwari, and Taufik, "Simulation of Modified Simple Boost Control for Z-Source Inverter", International Journal of Automation and Power Engineering (IJAPE), Volume 2, Issue 4, Pp. 57-64, 2013.
- [11] Vrushali Suresh Neve, P.H. Zope, and S.R. Suralkar, "Analysis and Simulation of Z-Source Inverter Fed to Single Phase Induction Motor Drive", International Journal of Scientific Engineering and Technology, Volume No.2, Issue No.1, pp : 08-12, 2013.
- [12] Quang-Vinh Tran, Tae-Won Chun, Jung-Ryol Ahn, and Hong-Hee Lee, "Algorithms for Controlling Both the DC Boost and AC Output Voltage of Z-Source Inverter", IEEE Transactions On Industrial Electronics, Vol. 54, No. 5, Pp. 2745-2750, 2007.